Development of Spectrally-Constrained Diffuse Optical Tomography for Imaging Exogenous Contrast Agents

Scott C. Davis, Brian W. Pogue, Subha Srinivasan, Hamid Dehghani, and Keith D. Paulsen
Thayer School of Engineering, Dartmouth College, Hanover NH 03755
(Email: scott.c.davis@dartmouth.edu, Tel:(603) 646-2230, Fax:(603) 646-3856)

Abstract: Spectrally-constrained diffuse tomography is used to image endogenous and exogenous tissue chromophore concentrations with higher accuracy than when using individual wavelengths. Reconstructed images from simulated data demonstrate that concentrations of Lutetium Texaphyrin are readily recovered.

OCIS codes: (170.3880) Medical and biological imaging; (170.6960) Tomography; (170.3830) Mammography

1. Introduction

Spectrally constrained reconstruction methods for diffuse optical tomography have been used to image endogenous tissue chromophore concentrations by incorporating a-priori spectral information directly in the inversion formulation. This technique, first demonstrated by Corlu et al. [1] and Li et al. [2] for reconstructing from continuous wave data, was expanded for frequency domain systems and shown to provide qualitatively and quantitatively accurate images of hemoglobin concentration, oxygen saturation, water content, and scattering amplitude and power [3, 4]. It is commonly believed that additional physiological information may be obtained by imaging the spatial concentration of an administered contrast agent. Fluorescence diffuse tomography has been shown to provide highly sensitive imaging and targeted fluorophores may help further characterize the physiological processes in a given region [5, 6]. Another approach is to exploit the absorption characteristics of the administered agent by extending the spectrally constrained imaging method to incorporate a-priori information about the exogenous dye. This work investigates the feasibility of using Lutetium Texaphyrin, (LuTex), as an absorption contrast agent. Preferential uptake of LuTex, has been shown in cancerous tumors and it has been extensively tested as a photodynamic therapeutic agent [7-10]. Its very strong absorption peak at 732nm makes it an attractive candidate for studying exogenous chromophore imaging.

2. Methods

The diffuse nature of near-infrared (NIR) photon propagation in biological tissue is the foundation of the model system used, presented here in the frequency domain:

$$\nabla \cdot D(\vec{r})\nabla\phi(\vec{r},\omega) - [\mu_a(\vec{r}) + i\omega/c]\phi(\vec{r},\omega) = -q_0(\vec{r},\omega) \tag{1}$$

where $\phi(\vec{r},\omega)$ is the photon field within the tissue; μ_a is the absorption coefficient; D is the diffusion coefficient defined which contains the scattering coefficient μ_s'; and ω is the modulation frequency of an isotropic source, q_0.

The theoretical formulation is an extension of the established technique which is used to image tissue concentration of oxygenated and deoxygenated hemoglobin, water content, scatter amplitude and scatter power, as described in [4]. The inversion is constrained by prior knowledge of the chromophore absorption spectra, and application of Beer's law

$$\mu_a(\lambda) = [\varepsilon(\lambda)]c \tag{2}$$

As well as by an empirical approximation to Mie Theory,

$$\mu_s' = a\lambda^b \tag{3}$$

Here, λ is wavelength, ε is the extinction coefficient, c is the chromophore concentration, a is the scatter amplitude, and b the scatter power. Frequency domain data measured for a range of laser source wavelengths can be coupled in the following manner

$$\partial\phi_\lambda = \Im_{c,\lambda}\partial c + \Im_{a,\lambda}\partial a + \Im_{b,\lambda}\partial b \tag{4}$$

where $\partial\phi$ is the change in boundary data and

$$\Im_{c,\lambda} = \frac{\partial\phi}{\partial\mu}\frac{\partial\mu}{\partial c}\bigg|_\lambda,\ \Im_{a,\lambda} = \frac{\partial\phi}{\partial\kappa}\frac{\partial\kappa}{\partial a}\bigg|_\lambda,\ \Im_{b,\lambda} = \frac{\partial\phi}{\partial\kappa}\frac{\partial\kappa}{\partial b}\bigg|_\lambda \tag{5}$$

Following Ref. [4], the system of equations are assembled;

$$\begin{pmatrix}\partial\phi_{\lambda 1}\\ \partial\phi_{\lambda 1}\\ \cdots\\ \partial\phi_{\lambda n}\end{pmatrix} = \begin{bmatrix}\Im_{c1,\lambda 1}\Im_{c2,\lambda 1}\Im_{c3,\lambda 1}\Im_{c4,\lambda 1}\Im_{a,\lambda 1}\Im_{b,\lambda 1}\\ \Im_{c1,\lambda 2}\Im_{c2,\lambda 2}\Im_{c3,\lambda 2}\Im_{c4,\lambda 2}\Im_{a,\lambda 2}\Im_{b,\lambda 2}\\ \cdots\\ \Im_{c1,\lambda n}\Im_{c2,\lambda n}\Im_{c3,\lambda n}\Im_{c4,\lambda n}\Im_{a,\lambda n}\Im_{b,\lambda n}\end{bmatrix}\begin{pmatrix}\partial c_1\\ \partial c_2\\ \partial c_3\\ \partial c_4\\ \partial a\\ \partial b\end{pmatrix} \tag{6}$$

where *c1*, *c2*, and *c3* indicate endogenous chromophores (oxy- and deoxy-hemoglobin concentration and water content). Here *c4* is incorporated to include an exogenous chromophore. In practice, contrast agent concentrations in-vivo are expected to be much lower than endogenous chromophore concentrations, thus administered contrast agents with large extinction coefficients are preferred to ensure that the drug's spectral features contribute to the overall tissue absorption spectrum. If the extinction coefficients are too low, the contrast agent has little impact on the overall absorption spectrum and images of drug concentration cannot be obtained readily. Preferably, the exogenous agent has a peak absorption that dominates a region of the overall tissue absorption spectra, even at low concentrations. LuTex is an ideal candidate for this technique due to its strong absorption peak at 732 nm.

Extinction coefficient values for LuTex[7] are shown in figure 1 along with the absorption spectra of endogenous chromophores.

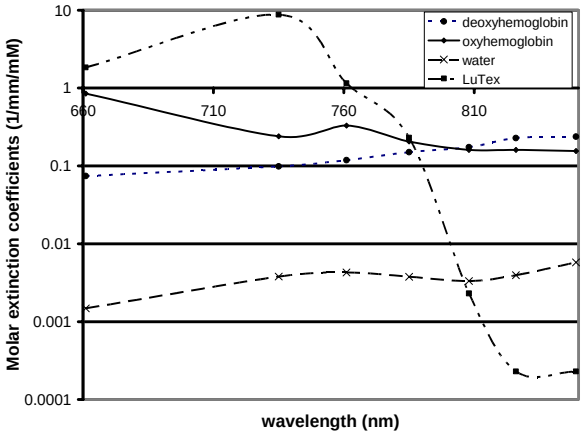

Figure 1. Absorption spectra of endogenous chromophores (measured directly) and LuTex (as reported by Ref. [7]).

The reconstruction algorithm recovers images of endogenous and exogenous chromophore concentration simultaneously. Six laser wavelengths spanning the NIR spectrum were used to image the endogenous

chromophores and scattering parameters in the previous frequency domain system. Adding a seventh wavelength at 735nm provides additional spectral information which can be used to image the spatial distribution of LuTex.

3. Results

Recovered images from simulated noisy data presented in figure 2 show total hemoglobin concentration, oxygen saturation, water content, LuTex concentration scattering amplitude and power. Frequency domain data was generated for 7 laser wavelengths, 661, 735, 761, 785, 808, 826, 849nm to match ongoing experimental work.

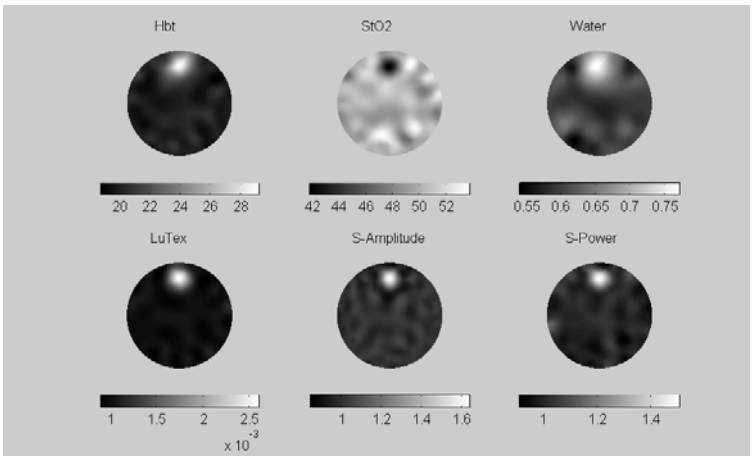

Fig. 2. Images of total hemoglobin concentration (in μM), oxygen saturation (%), water content (%), lutetium texaphyrin concentration (mM), scatter amplitude and scatter power reconstructed from simulated noisy data. True values of LuTex concentration were 0.001 mM in the background and 0.003 in the anomaly

4. Discussion

Reconstructed images show that images of exogenous contrast agent concentration are readily recovered along with endogenous chromophore concentrations using the spectrally constrained reconstruction technique. The LuTex images demonstrate good qualitative and quantitative agreement with true values for the cases tested. LuTex has been shown to preferentially accumulate in some forms of carcinoma, and therefore may offer an additional physiological descriminator in the form of a temporal contrast agent in the tumor site.

This work is funded by NIH grants RO1CA69544 and U54CA105480.

5. References

[1] A. Corlu, T. Durduran, R. Choe, M. Schweiger, E. M. Hillman, S. R. Arridge, and A. G. Yodh, "Uniqueness and wavelength optimization in continuous-wave multispectral diffuse optical tomography," *Optics Letters*, vol. 28, pp. 2339-2341, 2003.

[2] A. Li, Q. Zhang, J. Culver, E. Miller, and D. Boas, "Reconstructing chromophore concentration images directly by continuous-wave diffuse optical tomography," *Optics Letters*, vol. 29, pp. 256-258, 2004.

[3] S. Srinivasan, B. W. Pogue, B. Brooksby, S. Jiang, H. Dehghani, C. Kogel, W. A. Wells, S. P. Poplack, and K. D. Paulsen, "Near-Infrared Characterization of Breast Tumors In Vivo using Spectrally-Constrained Reconstruction," *Technology in Cancer Research and Treatment*, vol. 4, pp. 513-526, 2005.

[4] S. Srinivasan, B. W. Pogue, S. Jiang, H. Dehghani, and K. D. Paulsen, "Spectrally Constrained Chromophore and Scattering Near-infrared Tomography Provides Quantitative and Robust Reconstruction," *Appl. Opt.*, vol. 44, pp. 1858-1869, 2005.

[5] E. Graves, J. Ripoll, R. Weissleder, and V. Ntziachristos, "A submillimeter resolution fluorescence molecular imaging system for small animal imaging," *Medical Physics*, vol. 30, pp. 901-911, 2003.

[6] V. Ntziachristos, C. Bremer, and R. Weissleder, "Fluorescence imaging with near-infrared light: new technological advances that enable in vivo molecular imaging," *European Radiology*, vol. 13, pp. 195-208, 2003.

[7] G. Kostenich, T. Babushkina, A. Lavi, Y. Langzam, Z. Malik, A. Orenstein, and B. Ehrenberg, "Photosensitization by the near-IR-absorbing photosensitizer lutetium texaphyrin: spectroscopic, in vitro and in vivo studies," *Journal of Porphyrins and Phthalocyanines*, vol. 2, pp. 383-390, 1998.

[8] G. Kostenich, A. Orenstein, L. Roitman, Z. Malik, and B. Ehrenberg, "In vivo photodynamic therapy with the new near-IR absorbing water soluble photosensitizer lutetium texaphyrin and a high intensity pulsed light delivery system," *Journal of Photochemistry & Photobiology B - Biology*, vol. 39, pp. 36-42, 1997.

[9] K. W. Woodburn, Q. Fan, D. R. Miles, D. Kessel, Y. Luo, and S. W. Young, "Localization and efficacy analysis of the phototherapeutic lutetium texaphyrin (PCI-0123) in the murine EMT6 sarcoma model," *Photochemistry & Photobiology*, vol. 65, pp. 410-5, 1997.

[10] S. W. Young, K. W. Woodburn, M. Wright, T. D. Mody, Q. Fan, J. L. Sessler, W. C. Dow, and R. A. Miller, "Lutetium texaphyrin (PCI-0123): a near-infrared, water-soluble photosensitizer," *Photochemistry & Photobiology*, vol. 63, pp. 892-7, 1996.